Supplemental Figure 1

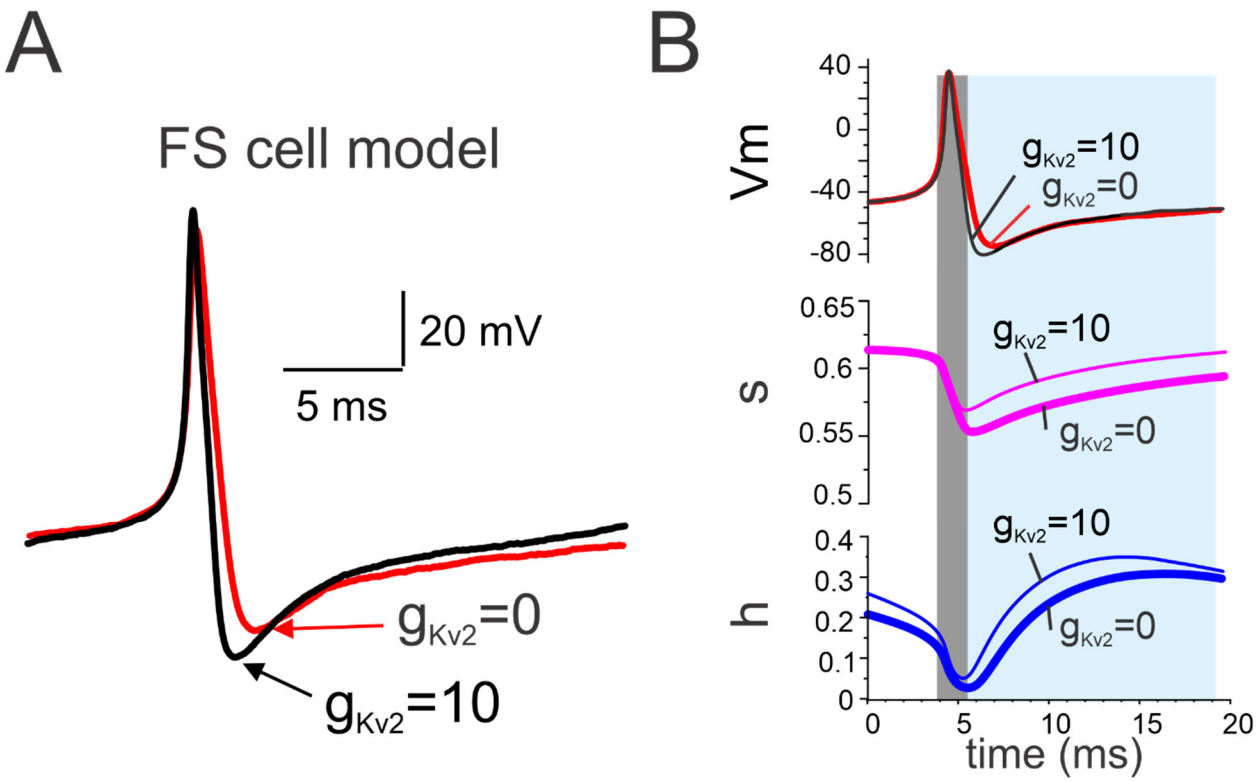

As observed in **A),** in the FS cell model with reduced g_{Kv2}, the afterhyperpolarization associated with single spikes had smaller amplitude, whereas the action potential repolarization was slower. Importantly, both the inactivation and the recovery from inactivation of Na^+ channels are time- and voltage-dependent, while, specifically, the recovery from inactivation requires a hyperpolarized potential. Hence, the reduction of the afterhyperpolarization amplitude may contribute to the mechanisms by which decreasing Kv2.1 conductance increases Na^+ channel inactivation, thus promoting stuttering. We therefore investigated whether changes in the afterhyperpolarization properties contribute to greater Na^+ channel inactivation. To assess inactivation, we examined in **B)** the time course of the inactivation gating variables, s and h, around the time window of an action potential. The time window of Na^+ channel inactivation by the action potential (gray rectangle in **B**) starts during the ascending/depolarization phase and reaches its maximum (lowest value of s or h) during the descending/repolarization phase. Then, the time window when Na^+ channels recover from inactivation (light blue rectangle in **B**) starts during the action potential descending/repolarization phase but largely coincided with the afterhyperpolarization. Hence, as a likely consequence of the slower action potential repolarization and smaller afterhyperpolarization amplitude, in the model with reduced g_{Kv2} the maximal inactivation of the Na^+ conductance was larger and the recovery from inactivation was slower, possibly explaining the temporal summation of inactivation during successive spikes (Figure 3F). Our simulations therefore suggest that greater inactivation and impaired recovery of Na^+ channels from inactivation, secondary to reduced Kv2.1-mediated currents, affect repetitive firing in FS cells.

Supplemental Figure 2

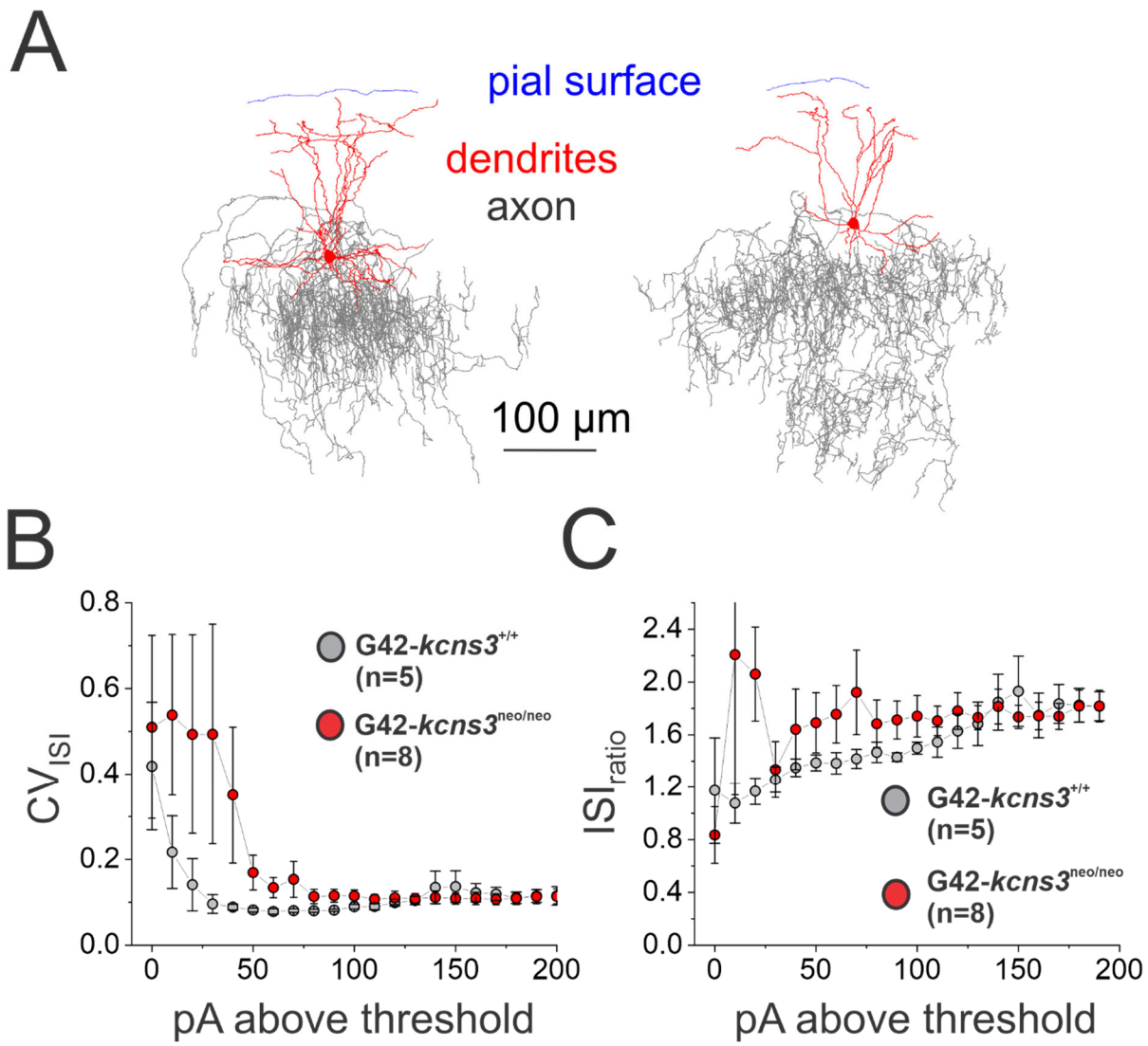

Examples of chandelier cells filled with biocytin in slices from G42-*Kcns3*$^{+/+}$ mice are shown in **A)** As show in the Figure, the chandelier cells had cell body located at a distance from the pial surface corresponding to the superficial portion of layer 2, consistent with our previous studies showing that chandelier cells have cell bodies exclusively localized near the border between layers 1 and 2 (Miyamae et al 2017; Tikhonova et al 2018). Figure **B)** depicts graphs of the coefficient of variation of the Inter-Spike Intervals (CV_{ISI}) (mean±SEM) computed for spike trains evoked by current steps in chandelier cells from G42-*Kcns3*$^{+/+}$ (n=5 cells) and G42-*Kcns3*$^{neo/neo}$ mice (n=8 cells). Mann-Whitney tests comparing the CV_{ISI} by genotype produced p≥0.0551 for current levels between 0 and 100 pA above threshold. Figure **C)** shows plots of the ratio of the last and first Inter-Spike Intervals (ISI_{ratio}) (mean±SEM) computed for spike trains evoked by current steps in chandelier cells from G42-*Kcns3*$^{+/+}$ (n=5 cells) and G42-*Kcns3*$^{neo/neo}$ mice (n=8 cells). Mann-Whitney tests comparing ISI_{ratio} by genotype produced p≥0.10789 for current levels between 100 and 200 pA above threshold.

Supplemental Figure 3

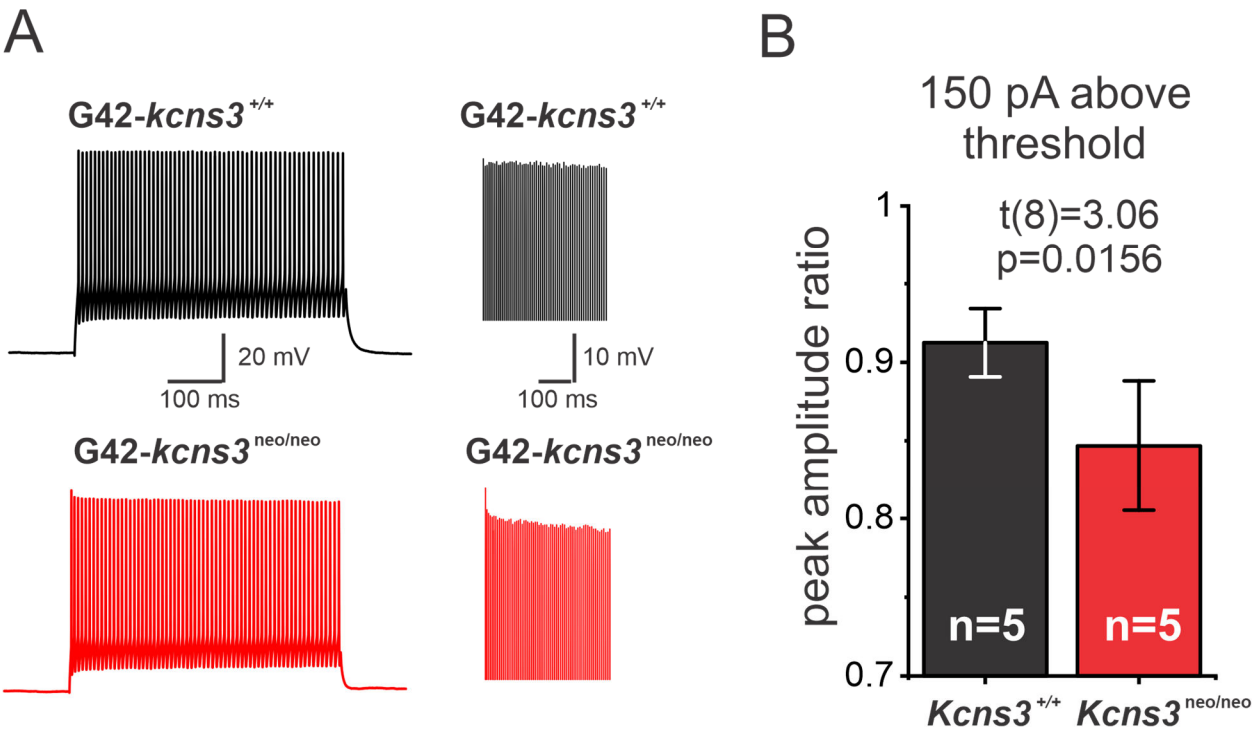

During repetitive firing with high stimulus current above threshold, action potentials in PVBCs show a small but consistent decrease in peak amplitude. As shown in **A**, this decrease in amplitude was stronger in PVBCs from *Kcns3*-deficient mice. The traces in the right panel of A, are shown truncated and at different voltage a time scales, to illustrate the changes in spike amplitude. The changes in action potential peak amplitude were quantified as the ratio between the amplitude of the first spike in a 50 ms window (placed at the end of the 500 ms current step) relative to the first action potential in the spike train. As shown in **B**, the ratio was significantly smaller in PVBCs from *Kcns3*-deficient mice. These changes in action potential peak amplitude are consistent with the findings of our computational modeling study (see Figure 3) suggesting that in PVBCs from *Kcns3*-deficient mice inactivation of Na+ channels, which influences action potential amplitude, is enhanced. When PVBCs were stimulated with currents closer to threshold, a similar decrease in action potential peak amplitude was observed in some but not all PVBCs (see Figure 6), irrespective of genotype, although the effect was more variable (data not shown).

Supplemental Figure 4.

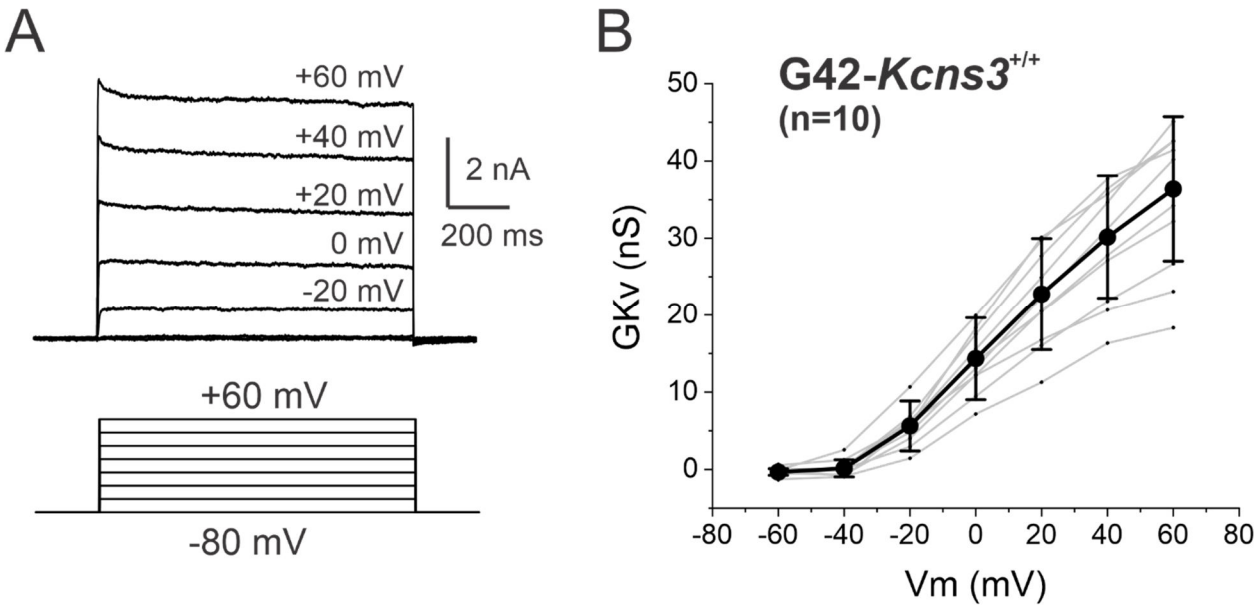

Supplemental Figure 4. Voltage-gated potassium currents recorded from PV neurons in brain slices display evidence of significant space clamp errors.

In order to evaluate whether Kv currents are affected by *Kcns3* deficiency, voltage clamp recordings are needed to test the two main predictions that can be made regarding the Kv currents in G42-*Kcns3*$^{+/+}$ versus G42-*Kcns3*$^{neo/neo}$ mice: 1) the voltage dependence of the Kv current should be shifted to the left in wild type neurons. 2) The maximal Kv conductance (GKv) should be larger in wild type neurons. Testing these two predictions requires assessing the plateau or saturation portion of the activation curve of the GKv, expected to be reached at membrane potentials of +40 mV and above, consistent with the known voltage dependence of Kv2.1 and Kv2.1-Kv9.3 currents. However, voltage clamp recordings performed in neurons in brain slices are predicted to involve significant voltage clamp errors that greatly distort the recorded Kv currents, precluding to assess the plateau region.

As shown in **A**, the recorded Kv currents had substantial amplitudes, reaching 3-10 nA in some cases. Whereas the large size of the Kv currents is consistent with their importance for PVBC physiology, their large amplitude may be associated with the significant voltage clamp errors that became evident during analysis of the activation of the Kv current by depolarizing pulses. Specifically, for voltage pulses farther away from the equilibrium potential for K^+ ions (E_{K^+}) the larger the amplitude of the elicited currents the greater the distorsion introduced by voltage clamp errors (Bar-Yehuda and Korngreen, 2008).

As show in **B**, the activation curve of the conductance indicated the presence of significant voltage clamp errors very similar to, and possibly larger than, those described by Bar-Yehuda and Korngreen 2008 (Bar-Yehuda and Korngreen, 2008). Specifically, the activation curve did not show a plateau for depolarizing commands of +40 and +60 mV, in marked contrast with Kv2-Kv9.3 or Kv2 currents recorded in the absence of space clamps errors. Gray lines represent individual PV neurons and the black lines are mean± SD (n=10, 2 mice).

Supplemental Methods

Recordings of voltage-dependent potassium currents

We performed voltage clamp recordings from PV neurons in slices from G42-*Kcns3*$^{+/+}$ mice, isolating Kv currents after blocking Na^+ and Ca^{2+} currents with tetrodotoxin (1 μM) and cadmium (1 μM), respectively. The pipette solution had the following composition (in mM): KGluconate 60, KCl 70, HEPES 10, EGTA 0.2, MgATP 4.5, NaGTP 0.3, sodium phosphocreatine 14, pH 7.2–7.4. When filled with this solution, pipettes had a resistance of 3-5 MΩ. Using a P/-4 protocol to subtract leak and capacitive currents, our procedure was similar to that employed by Guan and colleagues (Guan et al., 2013) to record Kv2 currents from pyramidal neurons in brain slices. As in Guan et al. 2013, we did not routinely employ series resistance or whole cell capacitance compensation. We elicited families of currents using 500 ms depolarizing steps from a holding potential of -80 mV. The depolarizing pulses were applied in 20 mV increments until reaching a nominal voltage of +60 mV. The currents elicited by the voltage pulses were measured at 200 or 300 ms from the onset of the voltage pulses, after subtracting the leak and capacitive currents using scripts written in OriginPro. The currents measured in the 200 or 300 ms time points produced nearly identical results and were averaged. The Kv conductance (GKv) was estimated by dividing the current by the driving force.

References

Bar-Yehuda, D., Korngreen, A., 2008. Space-clamp problems when voltage clamping neurons expressing voltage-gated conductances. J Neurophysiol. 99**,** 1127-36.

Guan, D., et al., 2013. Kv2 channels regulate firing rate in pyramidal neurons from rat sensorimotor cortex. J Physiol. 591**,** 4807-25.